IOP Publishing Journal of Physics D: Applied Physics
J. Phys. D: Appl. Phys. **46** (2013) 185101 (6pp) doi:10.1088/0022-3727/46/18/185101

Graphene geometric diodes for terahertz rectennas

Zixu Zhu, Saumil Joshi, Sachit Grover[1] and Garret Moddel

Department of Electrical, Computer, and Energy Engineering, University of Colorado, Boulder, CO 80309-0425, USA

E-mail: moddel@colorado.edu

Received 30 November 2012, in final form 15 March 2013
Published 15 April 2013
Online at stacks.iop.org/JPhysD/46/185101

Abstract
We demonstrate a new thin-film graphene diode called a geometric diode that relies on geometric asymmetry to provide rectification at 28 THz. The geometric diode is coupled to an optical antenna to form a rectenna that rectifies incoming radiation. This is the first reported graphene-based antenna-coupled diode working at 28 THz, and potentially at optical frequencies. The planar structure of the geometric diode provides a low RC time constant, on the order of 10^{-15} s, required for operation at optical frequencies, and a low impedance for efficient power transfer from the antenna. Fabricated geometric diodes show asymmetric current–voltage characteristics consistent with Monte Carlo simulations for the devices. Rectennas employing the geometric diode coupled to metal and graphene antennas rectify 10.6 μm radiation, corresponding to an operating frequency of 28 THz. The graphene bowtie antenna is the first demonstrated functional antenna made using graphene. Its response indicates that graphene is a suitable terahertz resonator material. Applications for this terahertz diode include terahertz-wave and optical detection, ultra-high-speed electronics and optical power conversion.

(Some figures may appear in colour only in the online journal)

1. Introduction

An optical rectenna incorporates an antenna and a diode to convert high-frequency electromagnetic fields to direct current (dc) power [1]. Figure 1 shows the configuration of an optical rectenna system, in which light is absorbed by an optical antenna and converted to alternating current (ac). An ultrafast diode rectifies the ac current to provide dc power to a load. The two primary requirements for the diode are ultra-high-speed response and an impedance that is well matched with that of the antenna. The most widely investigated diode for terahertz rectennas is the metal–insulator–metal (MIM) diode, which is limited in frequency response because of fundamental RC constraints in parallel-plate devices [2]. We propose and demonstrate a new type of diode, called a geometric diode, that does not suffer from the RC constraints of parallel-plate devices because of its planar structure. Because it is formed from a conductive material, the resistance of the geometric diode is also sufficiently low to match the antenna impedance [3].

[1] Present address: National Center for Photovoltaics, National Renewable Energy Lab., Golden, CO 80401, USA.

2. Principle of operation

The fundamental physical requirement for the geometric diode is that its critical dimensions are on the order of the mean-free path length (MFPL) of charge carriers in the material. On this scale, the charge carrier transport within the diode can be considered ballistic, such that the boundaries and the geometry of the device have substantial impact on the charge movement [4]. High-frequency ballistic devices operating at 50 GHz based on geometric asymmetry in semiconductors have been demonstrated [5]. In contrast, the geometric diode is formed from a conductive material which supplies the ballistic charge carriers. We chose graphene as the thin-film material because its MFPL is significantly greater than that of metals. This allows for devices that are sufficiently large to be fabricated within the capabilities of current lithography techniques. Furthermore, as we shall see, the limiting frequency for charge transport in graphene is higher than what has been obtained in semiconductors [6].

The operation of a geometric diode is shown in figure 2(*a*). The critical region of the device is the inverse

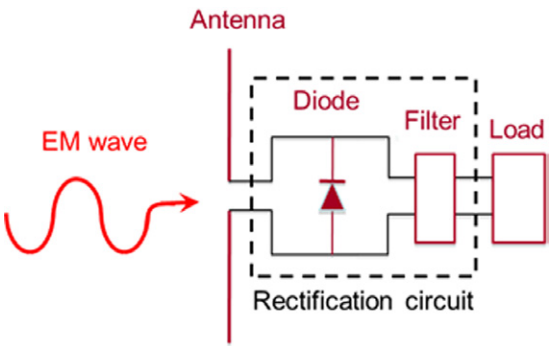

Figure 1. Schematic of a rectenna. An incident electromagnetic wave is received by the antenna, and rectified by the circuit containing diode and a low-pass filter, providing a dc voltage to the load.

arrowhead-shaped constriction (the neck region). The left-to-right moving carriers have a higher probability of reflecting off the diagonal walls on the left-hand side of the neck and channelling through the arrowhead region than the right-to-left moving carriers, which are more likely to be blocked by the flat walls on the right-hand side of the arrowhead. This difference in probability causes dissimilar current levels for forward (driving left-to-right motion) and reverse (driving right-to-left motion) bias voltages. An atomic force microscope (AFM) image of a fabricated device is shown in figure 2(*b*).

3. Monte Carlo simulation

The current–voltage ($I(V)$) asymmetry of the diode was modelled using a Monte Carlo simulation based on the Drude model to simulate the movement of charge within the device [7]. In the simulation, the charges have a randomly directed Fermi velocity within each collision time and reflect specularly at the edges of the device. The Fermi velocity of charge carriers in graphene was calculated to be about $10^6\,\mathrm{m\,s^{-1}}$ based on a backscattering MFPL of 45 nm, corresponding to a collision time of 5×10^{-14} s. The MFPL was experimentally determined from the conductivity versus gate voltage measured in a region adjacent to the diode [8]. The backscattering MFPL was obtained by multiplying the elastic MFPL by $\pi/2$, which is an averaging factor for scattering in two dimensions. Because the backscattering MFPL—as opposed to the elastic MFPL—is a closer approximation to the inelastic MFPL used in the Drude model, it is the number that we have used in the simulation [9]. The simulation uses a carrier concentration of $1.1\times10^{12}\,\mathrm{cm^{-2}}$, which is the value determined from the conductivity versus gate voltage measurement for a gate voltage of 30 V. When a simulated dc voltage is applied, a constant field velocity is added to the thermal velocity based on a charge effective mass of $0.02m_\mathrm{e}$ in graphene [10], where m_e is the electron rest mass. Although the field velocity is small compared with the Fermi velocity, a low-noise $I(V)$ curve shown in figure 3 was obtained after running the program for a sufficiently long time corresponding to approximately 10^6 collisions. The width of the neck and device geometric asymmetry determine the $I(V)$ asymmetry. Shrinking the neck width while keeping all other device dimensions the same increases the $I(V)$ asymmetry, as shown in figure 3. The MFPL is the key material parameter used in the simulation, and is assumed to be 200 nm, a typical value for high-quality graphene.

4. Material and fabrication

The material used to fabricate the geometric diode must meet two requirements. The first is the ability to withstand high current density through the neck, up to $10^7\,\mathrm{A\,cm^{-2}}$. This number comes from the value of V_DS required to observe asymmetry in the $I(V)$ characteristic. For metal devices, this V_DS is on the order of 0.1 V. Assuming the device has a 100 Ω matched resistance to antenna, the current density in the neck region with a cross section area of $100\times100\,\mathrm{nm^2}$ is $10^7\,\mathrm{A\,cm^{-2}}$. The second requirement of the material is a sufficiently large charge carrier MFPL. Being a planar conductive thin-film device, metal was our initial choice. However, the MFPL of charge carriers in metals at room temperature is 10–30 nm [7], which would necessitate impractically small neck geometries. Furthermore, we found that at high current densities metals with small junctions suffer from electromigration. To circumvent these disadvantages we incorporated graphene instead. Graphene devices working at terahertz have been shown theoretically and also demonstrated [11–13]. The MFPL in graphene can be up to 1 μm, corresponding to a carrier mobility of $200\,000\,\mathrm{cm^2\,V^{-1}\,s^{-1}}$ [14]. Graphene can withstand a current density of up to $10^8\,\mathrm{A\,cm^{-2}}$ [14].

We used mechanical exfoliation to apply graphene flakes onto an oxidized silicon substrate [8], consisting of a thermally grown 90 nm SiO_2 layer on a silicon wafer having a resistivity of 1–5 Ω cm. The diode electrodes were formed in a four-point-probe configuration [15] to avoid the effects of contact resistance. Dc $I(V)$ measurements were carried out by measuring the voltage drop between the inner contacts while applying a current through the outer contacts. The metal contacts (15 nm Cr/40 nm Au) were thermally evaporated and lifted off from an NR9-1000P photo resist. Electron-beam lithography (JEOL JBX-9300FS E-beam writer) on a ma-N negative E-beam resist followed by an oxygen plasma etch was used to pattern the graphene. The neck width was approximately 75 nm, with the MFPL measured to be ∼45 nm [9]. To prevent heating of the graphene and hysteresis due to charge build-up [16], a pulsed voltage was applied to the outer contacts using a Keithley 2612 SourceMeter set to the four-wire mode.

The conic band structure of graphene allows the carrier concentration to be controlled by the gate voltage. The charge neutral point (CNP) occurs for a gate voltage at which the electron and hole concentrations are equal, corresponding to a conductivity minimum. The substrate formed the gate. For our graphene, the CNP was obtained for a gate voltage of 24 V, as shown in figure 4. The suppression of the current at 0 V gate voltage indicates that the graphene has a small mesoscopic CNP inhomogeneity [17–19]. When the gate voltage is below the CNP voltage, holes are the majority charge carriers, and for gate voltages above the CNP voltage, electrons are the majority charge carriers. Because the forward direction in geometric

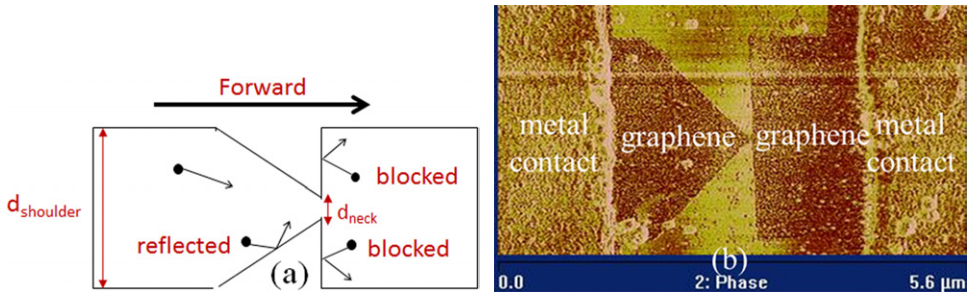

Figure 2. (*a*) Inverse arrowhead geometric diode structure. The neck width (d_{neck}) must be on the order of the MFPL for charge carriers in the material. The charge carriers reflect at the boundaries of the device. On the left-hand side of the neck, the carriers moving to the right can either directly channel through the neck or reflect off the tapering edges and keep moving forward. On the right-hand side of the neck, the vertical edge blocks most of the carriers moving to the left. Hence the diode forward direction for carriers is left-to-right. (*b*) AFM image of a fabricated graphene geometric diode device. The graphene inverse arrowhead diode is positioned between two metal contacts. Based on AFM scans the thickness of graphene is between 0.5 and 1 nm. The measured thickness is larger than the ideal 0.35 nm and is due to the AFM calibration and surface roughness of the substrate. The neck width is 75 nm.

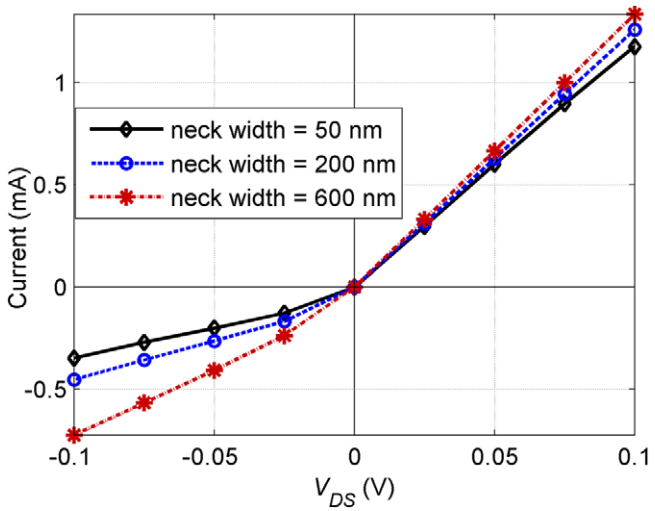

Figure 3. Simulated $I(V)$ curves for a geometric diode with different neck widths for a fixed shoulder width of 1 μm. Narrower necks restrict the reverse current more effectively. For V_{DS} value of 0.1 V the charge carrier drift velocity is 2.2×10^4 m s^{-1}, which is about 2% of the graphene electron Fermi velocity.

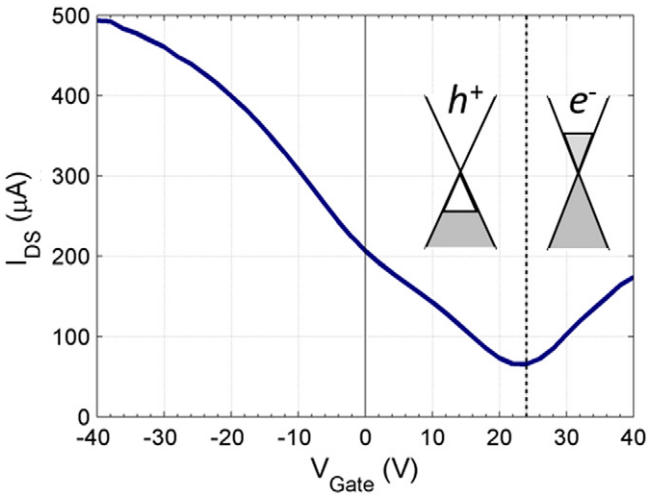

Figure 4. Dirac curve of the geometric diode made by exfoliated graphene. The CNP is around 24 V. Using the gate field effect method, we estimate the MFPL of this graphene piece to be ~45 nm.

diodes depends only on the geometry and is independent of carrier type, applying a gate voltage to change the dominant carrier type should reverse the polarity of the diode. This is, in fact, the case and it serves as confirmation that the rectification is due to the geometry [9].

5. 28 THz optical response

To test the high-frequency operation of the geometric diode, we formed a rectenna with a 5.1 μm long bowtie antenna in an edge-fed configuration [20]. The structure is a combination of two opposing 2.3 μm long triangular sections with a 500 nm long geometric diode placed at the center of the gap, as shown in figures 5(*a*) and (*b*). Devices with both metal (15 nm/45 nm thermally evaporated Cr/gold) and graphene antennas were fabricated. Figure 6 shows the setup of the optical measurement system at different polarization angles of the beam relative to the metal antenna/graphene geometric

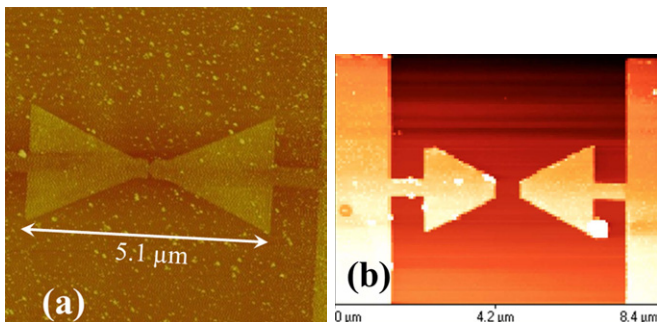

Figure 5. Geometric diode rectennas. AFM images of geometric diodes coupled to (*a*) a graphene and (*b*) a metal bowtie antenna. Because the metal antenna is so much thicker than the graphene diode in (*b*), the graphene cannot be seen in the AFM image.

diode rectenna system. An infrared CO_2 laser, operating at a wavelength of 10.6 μm and chopped at 280 Hz, was used as the source to measure rectification at optical frequencies. Two-point measurements were performed on the antenna-coupled diodes. The voltage and the current were measured separately using a lock-in amplifier with zero applied bias.

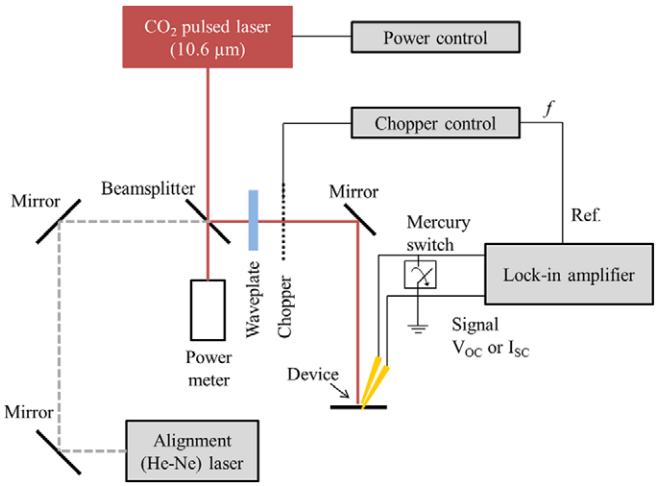

Figure 6. Rectenna optical measurement setup. The CO_2 laser beam was chopped at a frequency of 280 Hz and guided to the device by means of a set of mirrors. A lock-in amplifier, with the chopping frequency as the reference, and a two-point-probe setup was used to measure the photocurrent.

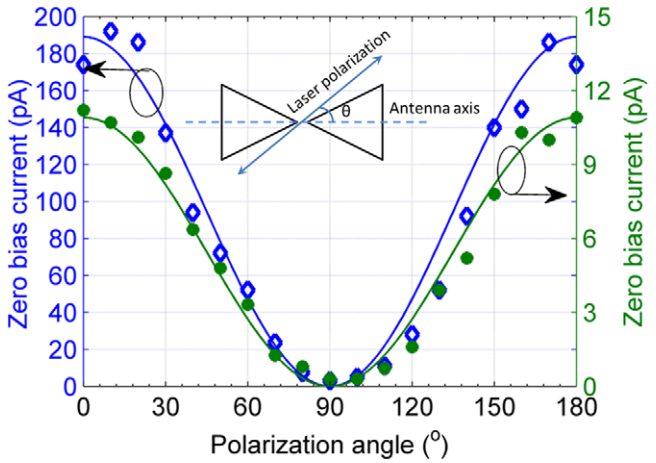

Figure 7. Short-circuit current response of a rectenna with a graphene antenna (green circles) and metal antenna (blue diamonds) as a function of polarization angle (θ). The graphene rectenna has a lower current response due to the larger series resistance of its antenna.

In figure 7 we show the diode short-circuit current as a function of beam polarization angle (θ) relative to the antenna axis for diodes coupled to metal and graphene antennas. The cosine squared response exhibited a maximum when the optical field and the antenna were aligned to each other, showing that the current was indeed produced by the radiation coupled through the antenna. When the laser polarization was aligned with the antenna axis, the output open circuit voltage was found to be proportional to the input optical laser power.

The rectenna with the graphene antenna exhibited a lower current response due to its much larger antenna series resistance, which is about 1 kΩ for the graphene antenna compared with a few ohms for the metal antenna. A recent simulation of graphene antenna at 1.4 THz indicates that to achieve high antenna response at terahertz the size of a graphene antenna needs to be much smaller than the metal antenna optimized for use at the same frequency [21]. Our antenna in figure 5(a) is probably too large to resonate at 28 THz, and might be more efficient if it were smaller.

This is the first reported graphene bowtie antenna working at terahertz frequency and it opens the possibility of using patterned graphene as an optical resonator. Bulk graphene absorbs 2.3% of incident white light [22]. Patterned graphene structures could enhance the light–plasmon coupling in graphene. Plasmon absorption of over 13% at 3 THz has been reported for graphene micro-ribbon arrays [10]. Since the graphene optical conductivity cutoff frequency is controlled by the gate voltage and intrinsic doping level [23], graphene antenna and resonators operating at terahertz frequencies can be competitive with conventional 2D resonators made of metal.

The angular dependence of the response indicates that rectification was not a result of optically generated charge diffusion or thermoelectric effects due to a difference in the illumination of the two sides of the junction. Also, no response was detected from an illuminated diode that was not coupled to an antenna. Since no gate voltage was applied to the antenna-coupled diodes before or during the measurement, no p–n junctions could have been formed as a result of an applied field [24]. The geometric diode genuinely responds to and rectifies 28 THz signals.

We compare the measured maximum current of 190 pA with the expected current as follows. Based on the measured laser beam power and beam width we estimate an input intensity of 5.6 mW mm^{-2} over an antenna area of approximately 37.5 μm^2 [25]. The diode/antenna coupling efficiency is calculated to be 12% [26] for a 3000 Ω diode and an antenna with a characteristic impedance of 100 Ω, and the antenna radiation efficiency is estimated to be 37% [25]. Although the bowtie antenna efficiency was poor, we chose it because of its relative ease of fabrication. The diode responsivity [3], which is defined as half the ratio of the second derivate to the first derivative of the $I(V)$ characteristic and is a measure of the dc power out divided by the ac power in, is a key figure of merit for rectenna operation. The zero-bias responsivity of the diode used in the rectenna optical measurement is 0.0285 A W^{-1}. Combining the estimated antenna parameters with the input power and the diode responsivity gives an estimated current of 270 pA, which is in good agreement with the measured value of 190 pA. A current of 190 pA for a wavelength of 10.6 μm corresponds to a quantum efficiency of 0.01%. Design improvements are expected to improve the antenna and diode efficiencies. In theory, a similar but smaller geometric diode (50 nm shoulder width with 10 nm neck width) has been shown to have more nonlinear and asymmetric $I(V)$ characteristics [27].

To calculate the capacitance we consider the fringing fields between the two sides of the geometric diode above the device in air and below in the 90 nm SiO_2 bottom substrate, and which induce charge storage. To estimate the worst case capacitance between the two sides of the neck, we assume that there is an approximately 100 nm by 100 nm air gap in the neck region. Using the planar thin-film capacitance analysis method [28] the capacitance of a graphene geometric diode is calculated to be about a few attofarads. The measured resistance of the graphene device is approximately 1 kΩ, which gives an overall

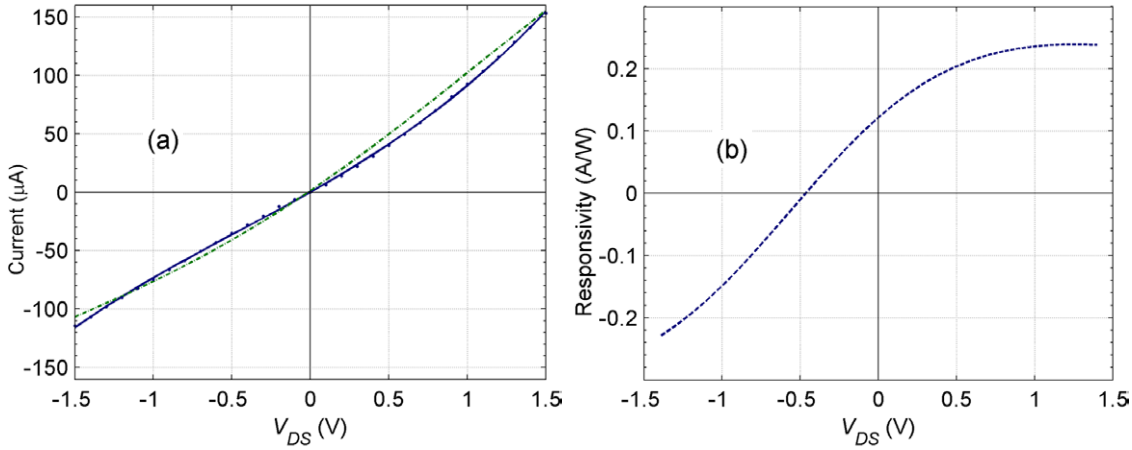

Figure 8. (*a*) Dc $I(V)$ characteristics (solid blue) for an exfoliated graphene geometric diode at a gate voltage of 20 V. The Monte Carlo simulation (dashed green) uses the dimensions of the fabricated device: neck width =75 nm, shoulder width =400 nm, and the measured MFPL =45 nm. (*b*) Calculated responsivity $[1/2|I''(V)/I'(V)|]$ as a function of the applied bias. At 0 V bias, the responsivity is 0.12 A W^{-1}.

RC time constant of femtoseconds corresponding to a cutoff frequency of 100 THz. By reducing the area of the non-critical region around the neck, the RC time constant can be reduced further.

6. Dc $I(V)$ measurements and verification of geometric effect

To investigate the relationship between the 28 THz and dc responses, we show the measured $I(V)$ curve for an exfoliated graphene diode in figure 8. The characteristics exhibit asymmetry in a direction that is consistent with simulation results obtained using the actual physical parameters of the device. A plot of the responsivity versus the applied voltage is shown in figure 8(*b*). This device has a responsivity of 0.12 A W^{-1} at zero bias voltage, and a responsivity over 0.2 A W^{-1} under bias. These diode parameters correspond to the measured stand-alone diode $I(V)$ characteristics, and are different from those of the antenna-coupled diode in figure 5. The responsivity is expected to improve substantially as the ratio of MFPL to neck width is increased, as shown in figure 3.

In graphene, $I(V)$ nonlinearity can be due to the graphene breaking down at a high voltage [29]. That is not the case here for two reasons. First, we have seen asymmetric nonlinearity at a low voltage not just at a high voltage. Second, the curvature of the reported nonlinearity of graphene at breakdown voltages had an opposite curvature direction compared with that of our diode $I(V)$ characteristics. At higher voltages, for $V_{DS} >$ 2.5 V, we found the diode $I(V)$ curvature starts to switch sign, possibly due to the breakdown phenomenon there.

To further confirm the effect of geometry on the $I(V)$ asymmetry, we compared the characteristics of geometrically symmetric and asymmetric junctions. We also fabricated asymmetric devices using graphene deposited by chemical vapour deposition (CVD) (provided by P L McEuen's laboratory at Cornell University) having a shorter MFPL than the exfoliated graphene devices. To quantify the $I(V)$ asymmetry we define the electrical asymmetry as $A = |I(V)/I(-V)|$. A comparison of the three devices is shown in figure 9. The value of

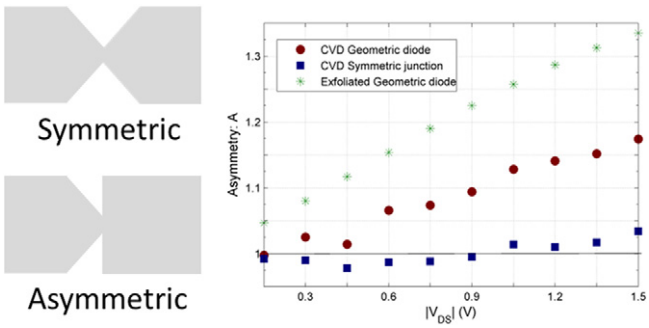

Figure 9. Electrical asymmetry plots for a CVD-produced graphene geometric diode (red circles), an exfoliated graphene geometric diode (green asterisks) and a geometrically symmetric CVD graphene junction (blue squares). The electrical asymmetry is defined as $A = |I(V)/I(-V)|$. CVD graphene, having a shorter MFPL than the exfoliated graphene, gives a lower asymmetry than the exfoliated graphene device. The neck width for all the devices is 75 nm, with a shoulder width of 400 nm.

A for a graphene geometrically symmetric junction remains at unity as compared with the geometrically asymmetric devices, which exhibit electrical asymmetry. The CVD graphene diode has a lower electrical asymmetry due to its reduced MFPL. The plot exhibits the significance of geometric asymmetry and the MFPL in achieving diode behaviour.

7. Conclusions

We have developed and demonstrated a new kind of diode for use in high-frequency rectennas. The graphene geometric diode exhibits dc $I(V)$ asymmetry and its measured electrical characteristics are consistent with Monte Carlo simulations. Rectennas incorporating geometric diodes provide optical frequency rectification of 10.6 μm wavelength radiation with both metal and graphene bowtie antennas. The measured short-circuit currents correspond to the values estimated using the diode and antenna parameters. Further improvement in the diode and antenna design is expected to increase device efficiency.

Acknowledgments

The authors gratefully acknowledge assistance in device preparation from Kendra Krueger and David Doroski. This work was carried out under a contract from Abengoa Solar, with initial support from Hub Lab. Device processing was carried out in part at the Colorado Nanofabrication Laboratory, and in part at the Cornell NanoScale Facility, both members of the National Nanotechnology Infrastructure Network, which is supported by the National Science Foundation (Grant ECS-0335765). We also thank Jonathan Alden in Professor P L McEuen's group in Cornell University for providing the CVD graphene sample.

References

[1] Fumeaux C, Herrmann W, Kneubühl F K and Rothuizen H 1998 *Infrared Phys. Technol.* **39** 123-83
[2] Grover S, Dmitriyeva O, Estes M J and Moddel G 2010 *IEEE Trans. Nanotechnol.* **9** 716-22
[3] Grover S and Moddel G 2011 *Solid State Electron.* **67** 94–9
[4] Datta S 1992 *Phys. Rev.* B **45** 13761–4
[5] Song A M 2002 *Appl. Phys.* A **75** 229–35
[6] Avouris P 2010 *Nano Lett.* **10** 4285–94
[7] Ashcroft N W and Mermin N D 1976 *Solid State Physics* (New York: Holt, Rinehart and Winston) chapter 1
[8] Novoselov K S *et al* 2004 *Science* **306** 666–9
[9] Nayfeh O M 2011 *IEEE Trans. Electron Devices* **58** 2847–53
[10] Ju L *et al* 2011 *Nature Nanotechnol.* **6** 630–4
[11] Ryzhii V 2006 *Japan. J. Appl. Phys.* **45** L923–5
[12] Rana F 2008 *IEEE Trans. Nanotechnol.* **7** 91–9
[13] Vicarelli L, Vitiello M S, Coquillat D, Lombardo A, Ferrari A C, Knap W, Polini M, Pellegrini V and Tredicucci A 2012 *Nature Mater.* **11** 865–71
[14] Castro Neto A H, Guinea F, Peres N M R, Novoselov K S and Geim A K 2009 *Rev. Mod. Phys.* **81** 109–62
[15] Moddel G, Zhu Z, Grover S and Joshi S 2012 *Solid State Commun.* **152** 1842–5
[16] Joshi P, Romero H E, Neal A T, Toutam V K and Tadigadapa S A 2010 *J. Phys.: Condens. Matter* **22** 334214
[17] Connolly M R, Chiou K L, Smith C G, Anderson D, Jones G A C, Lombardo A, Fasoli A and Ferrari A C 2010 *Appl. Phys. Lett.* **96** 113501
[18] Blake P, Wang R, Morozov S V, Schedin F, Ponomarenko L A, Zhukov A A, Nair R R, Grigorieva I V, Novoselov K S and Geim A K 2009 *Solid State Commun.* **149** 1068–71
[19] Lohmann T, von Klitzing K and Smet J H 2009 *Nano Lett.* **9** 1973–79
[20] Weiss M D, Eliasson B J and Moddel G 2003 *Patent* No 6664562
[21] Tamagnone M, Gomez-Diaz J S, Mosig J R and Perruisseau-Carrier J 2012 *J. Appl. Phys.* **112** 114915
[22] Nair R R, Blake P, Grigorenko A N, Novoselov K S, Booth T J, Stauber T, Peres N M R and Geim A K 2008 *Science* **320** 1308
[23] Li Z Q, Henriksen E A, Jiang Z, Hao Z, Martin M C, Kim P, Stormer H L and Basov D N 2008 *Nature Phys.* **4** 532–5
[24] Williams J R, DiCarlo L and Marcus C M 2007 *Science* **317** 638–41
[25] González F J and Boreman G D 2005 *Infrared Phys. Technol.* **46** 418–28
[26] Sanchez A, Davis C F Jr, Liu K C and Javan A 1978 *J. Appl. Phys.* **49** 5270
[27] Dragoman D and Dragoman M 2013 *J. Phys. D: Appl. Phys.* **46** 055306
[28] Zubko O G, Nikol'Skii S P and Vendik M A 1999 *Tech. Phys.* **44** 349–55
[29] Murali Y, Yang Y, Brenner K, Beck T and Meindl J D 2009 *Appl. Phys. Lett.* **94** 243114